12th International Workshop on Wave Hindcasting and Forecasting, Kohala Coast, Hawaii, HI, 2011.

ESTIMATION OF BREAKING CREST DENSITY AND WHITECAP COVERAGE FROM A NUMERICAL WAVE MODEL

Fabien Leckler[1]
Fabrice Ardhuin[2]
Nicolas Reul[3]
Bertrand Chapron[4]

IFREMER, Centre de Brest
Laboratoire d'Oceanographie Spatiale
Plouzane, FRANCE

Jean-François Filipot[5]

Service Hydrographique et Océanographique de la Marine
Brest, FRANCE

1 Introduction

Breaking waves play an important role at the air-sea interface, contributing to the surface hydrodynamic roughness, producing air bubbles into the water and sea spray in the atmosphere. Bubbles and foam alter the spectral reflectance and roughness of the ocean surface, with a strong signature in remotely sensed ocean properties [Reul and Chapron, 2003].

Wave breaking is also the main sink of the wave energy balance equation used in spectral wave models. Whereas early parameterizations essentially treated dissipation as a tuning knob for adjusting the wave model results, recent developments are striving to establish the parameterizations on physical grounds [see WISE Group, 2007, for a review]. Tolman and Chalikov [1996], introduced a separation of the dissipation source term into swell dissipation $S_{\rm sw}$ resulting in the effects of friction at air-sea interface [Ardhuin et al., 2009] and dissipation from breaking waves $S_{\rm br}$. Here we investigate the parameterization of the breaking wave dissipation term, that we split into a spontaneous breaking: waves that are steep enough to break by themselves, and an 'induced' or 'cumulative' breaking term. This decomposition is similar to that proposed by Young and Babanin [2006]. The cumulative term should include both the effect of modulations of short waves which can be made steep enough to break, and the wiping out of the short waves by longer breaking waves [Banner et al., 1989]. Here we only consider explicitly this second effect.

After discussing two parameterizations already used, in section 2, we will present in section 3 some modifications to the parameterization by Filipot [2010] with the objective to make it more realistic and self-consistent. In section 4 these parameterizations are used to estimate whitecap statistics in a realistic hindcast of the global ocean, using the foam time persistence model of Reul and Chapron [2003]. Conclusions and perspectives follow in section 5.

[1] E-mail:fabien.leckler@ifremer.fr
[2] E-mail:fabrice.ardhuin@ifremer.fr
[3] E-mail:nicolas.reul@ifremer.fr
[4] E-mail:bertran.chapron@ifremer.fr
[5] E-mail:jfilipot@shom.fr

2 Previous parameterizations

2.a Spontaneous Breaking: Parameterizations that are local in frequency

Banner et al. [2000] propose a wave group breaking probability as a function of wave steepness at spectral peak ϵ defined as $\epsilon = H_p k_p/2$, where $H_p = 4\sqrt{\int_{0.7f_\mathrm{p}}^{1.3f_\mathrm{p}} F_\mathrm{ws}(f).\mathrm{d}f}$ and F_ws is the wind sea spectrum. An empirical fit of dominant breaking probability P_B as function of wave steepness at spectral peak was found by the author such that $P_\mathrm{B}(\epsilon) = 22.0(\epsilon - 0.055)^{2.01}$.

In the same way, van der Westhuysen et al. [2007] proposed to use a direction-integrated saturation spectrum $B(k)$ and a threshold value B_r to estimate an isotropic breaking wave dissipation $S_{br}(k)$ such that:

$$B(k) = \int_0^{2\pi} k^3 F(k,\theta').\mathrm{d}\theta' \ , \quad S_{br} \sim \left[\frac{B(k)}{B_\mathrm{r}}\right]^{p/2} \tag{1}$$

with $B_\mathrm{r} = 1.2 \times 10^{-3}$ and p depended on wind friction velocity u_* and the degree of saturation $B(k)/B_\mathrm{r}$.

Following in this direction, Ardhuin et al. [2010] removed the strong wind speed dependence that was used in van der Westhuysen et al. [2007], based on the idea that the breaking is dominated by the wave geometry and that the wind plays a minor role [Banner et al., 2000]. Ardhuin et al. [2010] also included a direction-dependent saturation in order to reproduce better the observed directional spreads, and a the combination of a spontaneous and an induced breaking dissipations, which is necessary in order to reproduce the balance in the tail [see also Banner and Morison, 2010]. Here we will use the 'TEST 441b' parameterization,as defined by Ardhuin et al. [2010], in the WAVEWATCH III $^{(R)}$model version 4.05, which is in development and built on the numerical concepts and code by Tolman [2008].

The spontaneous breaking dissipation $S_\mathrm{bk,sp}$ is estimated using a saturation $B'(k,\theta)$ partially integrated over directions

$$\begin{aligned} B'(k,\theta) &= \int_{\theta-\Delta_\theta}^{\theta+\Delta_\theta} k^3 \cos^2(\theta-\theta') F(k,\theta') \frac{C_g}{2\pi} \mathrm{d}\theta' \\ B(k) &= \max\{B'(k,\theta), \theta \in [0, 2\pi[\} \end{aligned} \tag{2}$$

with $\Delta_\theta = 80$. The breaking probability is not zero when the saturation spectrum exceed and threshold value $B_r = 0.0009$, and the spontaneous dissipation is defined as a weighted combination of an isotropic dissipation and a direction-dependent term,

$$\begin{aligned} S_\mathrm{bk,sp}(k,\theta) = \sigma \frac{C_\mathrm{ds}^\mathrm{sat}}{B_r^2} \big\{ \delta_d \max[B(k) - B_r, 0]^2 + \\ (1-\delta_d) \max[B'(k,\theta) - B_r, 0]^2 \big\} \end{aligned} \tag{3}$$

where δ_d is the isotropy parameter which allows some control on the spectral directional spreading, here $\delta_d = 0.3$. $C_{\mathrm{ds}^{sat}}$ is adjusted to 2.2×10^{-4}.

2.b Spontaneous Breaking: parameterization based on wave scales

Because the saturation level varies rapidly with frequency around the peak, the parameterizations by van der Westhuysen et al. [2007] and Ardhuin et al. [2010] give a strongly varying dissipation rate that is not physical. Indeed, as underlined by Phillips [1984], most energy in a breaker is lost in a fraction r of the wave period, hence the spectral width of the dissipation compared to the carrier wave frequency should be proportional to $1/r$, which means a relatively broad distribution.

In order to be closer to the physical process of breaking, Filipot [2010] defined wave scales with finite frequency bandwidths, and estimated the heights of waves from a convolution of the wave spectrum Filipot et al. [2010]. This approach is consistent with observed Breaking Wave Height Distributions (BWHDs). Following Thornton and Guza [1983], the BWHD was parameterized as the product of the Rayleigh distribution of all wave heights (breaking or not) $P_\mathrm{R}(H)$ times a weight function $W(H)$ which the integration over wave height should provide the breaking probability for the wave field.

These breaking probabilities were then used to estimate a spectral dissipation rate [Filipot, 2010]. The benefit of that approach, among others, is that it allowed a natural transition from deep water 'whitecapping' into shallow water 'depth-induced breaking'. The parameterization adjusted to both surf zone and global scales is called here 'TEST 500'. Several wave scales are defined with a moving of a rectangular window $U_{\mathrm{Rec},f_\mathrm{c}}(f)$, applied over the direction-integrated spectrum $E(k)$. For each wave scale, Filipot [2010] defined representative wave heights H_{f_c}, wavenumber $\overline{k}_{f_\mathrm{c}}$, Rayleigh distributions $P_{\mathrm{R},f_\mathrm{c}}$ and weight functions W_{f_c}. For each wave scale the dissipation rate ϵ_{f_c} is given by the integral of $\epsilon_{f_\mathrm{c}}(H)$ over the distribution of wave heights H. Therefore, spontaneous breaking dissipa-

tion $S_{\mathrm{bk,sp},f_\mathrm{c}}$ for wave scale defined by f_c is

$$S_{\mathrm{bk,sp},f_\mathrm{c}} = \int_0^\infty W_{f_\mathrm{c}}(H) P_{\mathrm{R},f_\mathrm{c}}(H) \epsilon_{f_\mathrm{c}}(H) \Pi_{f_\mathrm{c}} dH \quad (4)$$

with $\Pi_{f_\mathrm{c}} = k/(2\pi\Delta_k)$ an estimation of the crest length by unit area in each rectangular windows.

The breaking dissipation $S_{\mathrm{bk,sp},f_\mathrm{c}}$ is then distributed over the wavenumber contained in the wave scale according with the energy distribution into the wave scale to obtain $S_{\mathrm{bk,sp},f_\mathrm{c}}(k)$. Due to the overlap of the filtering windows, each spectral component participates in several scales and the final spontaneous breaking dissipation $S_{\mathrm{bk,sp}}(k)$ for the waves with wavenumber k is an average of the $S_{\mathrm{bk,sp},f_\mathrm{c}}(k)$ obtained for the wave scales involving k. A distribution consistent with the directional distribution of energy for each wavenumber component is then applied to obtain a directional spontaneous breaking dissipation.

2.c Induced Breaking Parameterization

Here we consider that short waves are induced to dissipate when they are run over by a large-scale breaker. In other words, this dissipation term represents the smoothing of the surface by big breakers with celerity c' that wipe out smaller waves of phase speed c. The theoretical model of Ardhuin et al. [2009] is briefly described here. The relative velocity of the crests is the norm of the vector difference, $\Delta_c = |c - c'|$, and the dissipation rate of short wave is simply the rate of passage of the large breaker over short waves, that is, the integral of $\Delta_c \Lambda(c) \mathrm{d}c$, where $\Lambda(c)\mathrm{d}c$ is the length of breaking crests per unit surface that have velocity components between c and $c_\mathrm{x} + \mathrm{d}c_\mathrm{x}$, and between cy and $c_\mathrm{y} + \mathrm{d}c_\mathrm{y}$ [Phillips, 1985].

Ardhuin et al. [2010] estimated the breaking probabilities from the empirical fits proposed by Banner et al. [2000]. Estimating that the dominant wave steepness of Banner et al. [2000] is $\epsilon(k,\theta) = 1.6\sqrt{B'(k,\theta)}$, and correcting for the difference between spectral and zero-crossing analysis, the breaking probability is

$$P_\mathrm{B}(k,\theta) = 28.4 \max[B'(k,\theta) - B_\mathrm{r}, 0]^2 \quad (5)$$

Breaking probability is the ratio of breaking waves to the total number of waves. With this approach the authors defined the spectral density of the crest length (breaking or not) per unit surface $l(k,\theta)$ such that $\int l(k,\theta)\mathrm{d}k\mathrm{d}\theta$ is the total length of all crests per unit surface, with a crest being defined as a local maximum of the elevation in one horizontal direction. Thus, they obtain the spectral density of the breaking crest length per unit surface.

$$\Lambda(k,\theta) = l(k,\theta) P(k,\theta) \quad (6)$$

with

$$l(k,\theta) = 1/(2\pi^2) \quad (7)$$

This induced dissipation instantly removes all the energy of waves with frequencies $f_\mathrm{short} > r_\mathrm{bk,cu} f_\mathrm{long}$, where f_long is the frequency of the longer wave that is breaking spontaneously. then the induced dissipation rate is simply given by the rate at which these shorter waves are taken over by larger breaking waves times the spectral density,

$$\begin{aligned} S_{\mathrm{bk,cu}}(k,\theta) &= C_{\mathrm{bk,cu}} F(k,\theta) \\ &\times \int_{f'=0}^{r_{\mathrm{bk,cu}} f} \int_0^{2\pi} \Delta_c \Lambda(f',\theta) \mathrm{d}\theta' \mathrm{d}f' \end{aligned} \quad (8)$$

As a result the effect of breaking waves accumulates from the low to the high frequency and this effect is similar to the cumulative dissipation used by Young and Babanin [2006]. Unfortunately there is no direct link between this cumulative term which is used in the TEST441b and TEST500 parameterization and their respective parameterizations for the spontaneous dissipation.

3 Induced Breaking Dissipation from BWHD

This inconsistency is the reason why we propose here a cumulative term estimated from the same ideas, namely eq. (8), but in a way consistent with the spontaneous dissipation introduced by Filipot [2010] in TEST500, namely his parameterization of the breaking probability P_B. A first adjustment of this parameterization is proposed here and will be called TEST558.

3.a Academic test case

We consider here an uniform infinite deep ocean with an uniform 10 ms^{-1} wind. The model is started from rest. The spectrum is discretized using thirty two frequencies and twenty four directions. The Discrete Interaction Approximation [Hasselmann et al.,

1985] is used to compute nonlinear interactions between spectral components. The model was run with parameterizations TEST441b, TEST500 and TEST558 for 48 hours.

Breaking probabilities given by the integration of BWHD (with TEST558) are higher at large scales compared to those estimated from the saturation (with TEST441b). As a result, the cumulative breaking term is much larger with TEST558 compared to TEST441b. This effect was compensated in TEST558 by reducing the cumulative coefficient C_{cu} in eq.(8) from -0.4 to -0.2, this provides realistic spectral levels in the tail, with a roll off between f^{-4} and f^{-5} (figure 2).

Increasing this cumulative dissipation term leads to lower spectral levels at the tail, and, because of the wave-supported stress dependence in the wind input [Janssen et al., 1992], lower levels also at the peak. Compared to TEST500, this effect was compensated by decreasing the spontaneous dissipation term via the breaking probability coefficient which is reduced from 0.185 in TEST500 to 1.5 in TEST558. The wind wind input coefficient β_{max} was increased to 1.8, which finally gives values of the input source term similar to WAM Cycle 4 (figure 1). For both TEST441b and TEST558, computed spontaneous breaking probability for $U_{10}/c_{\mathrm{p}} \sim 1$ are presented in figure 3. Contrary to TEST441b and TEST500, the dissipation in the spectral tail with TEST558 is dominated by the cumulative breaking source term.

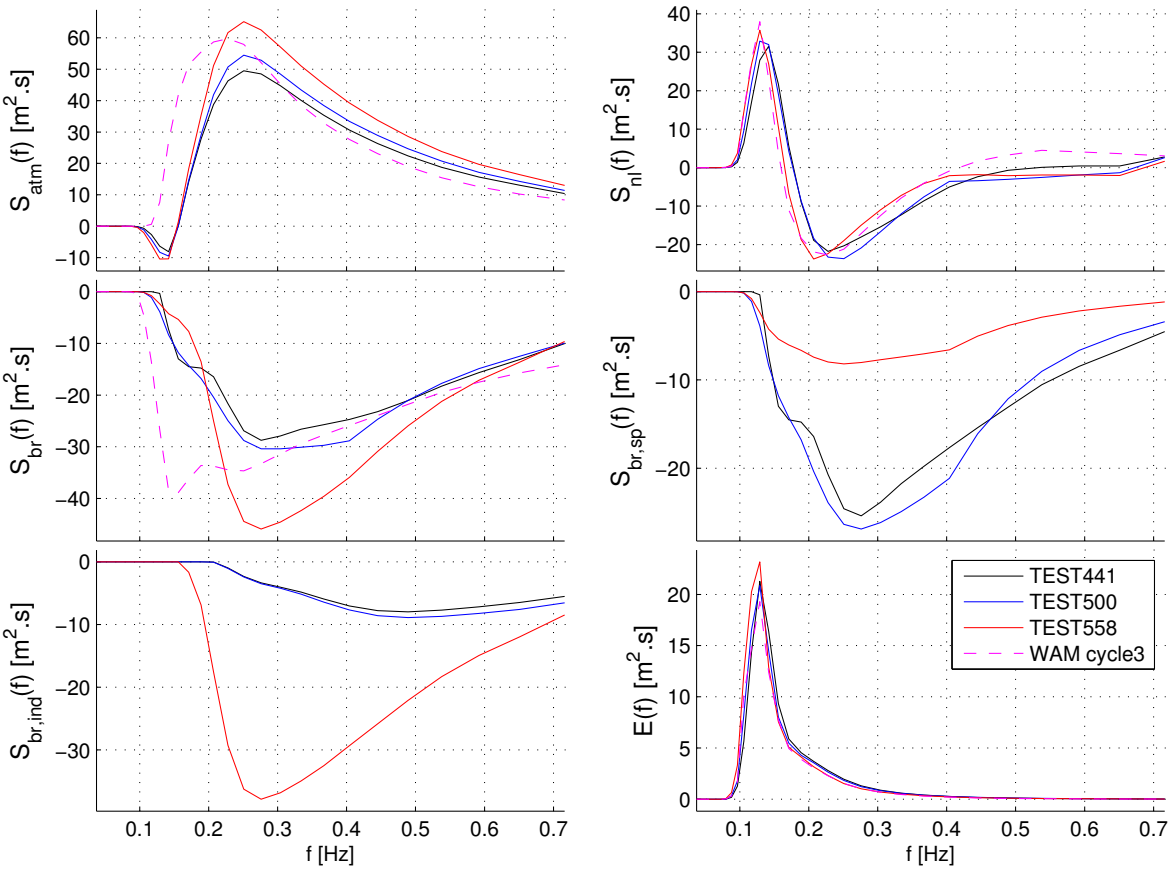

Fig. 1 : Sources term and spectrum for academic test case over a uniform deep ocean with a uniform 10 m s^{-1} wind starting from rest, after 8h of integration. Source term balances are given by the parameterization TEST441b, TEST500 and TEST558.

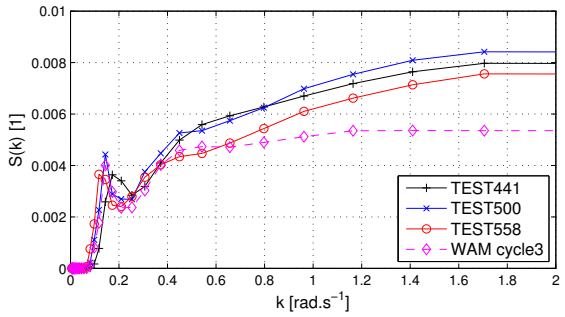

Fig. 2 : Saturation spectra obtained for an uniform infinite deep ocean with an uniform 10ms^{-1} wind after 48 hour of run, when $U_{10}/c_{\mathrm{p}} \sim 1$.

Time integrated source terms are shown in figure 1. Because of breaking probabilities from integration of BWHD are computes for overlapped wave scales, TEST500 and TEST558 have smoother spontaneous breaking source term than breaking dissipation from saturation spectrum (TEST441b). Although TEST441b and TEST500 had similar values for all source terms, the wind input in TEST558 is significantly larger, and balances a large dissipation term. This also leads to a faster growth of young waves ($U_{10}/c_{\mathrm{p}} < 1$).

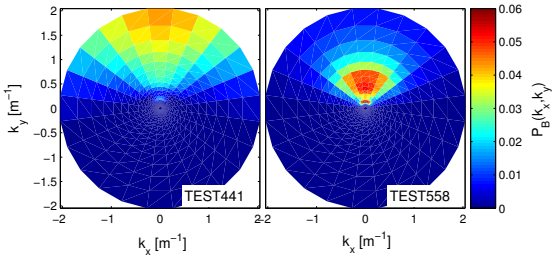

Fig. 3 : Spontaneous breaking probabilities from saturation spectrum (TEST441b,left plot) and ones from BWHD integration (TEST558,right plot) obtained for an uniform infinite deep ocean with an uniform 10ms^{-1} wind after 48 hours of run, when $U_{10}/c_{\mathrm{p}} \sim 1$

3.b Global hindcast

We also compare model runs with the different parameterizations to satellite altimeter data from Envisat, Jason 1 and Jason 2 for whole 2009 year (figure 4), using the Globwave cross-calibrated satellite database [Queffeulou and Croizé-Fillon, 2010]. The TEST558 run gives slightly larger errors than TEST441b, and may be improved by further adjustment. However, the results are still more accurate than using either WAM-Cycle 4 or the parameterization by Bidlot et al. [2005]. As expected from the faster growth of young waves, the low bias of TEST441b along east coasts is reduced in TEST558, giving lower errors. More problematic is the high bias for very large waves. Given that high wind speeds are generally underestimated in ECMWF analyses, using other wind fields, such as NCEP analyses or the CFSR reanalysis will produce even larger biases [Ardhuin et al., 2011].

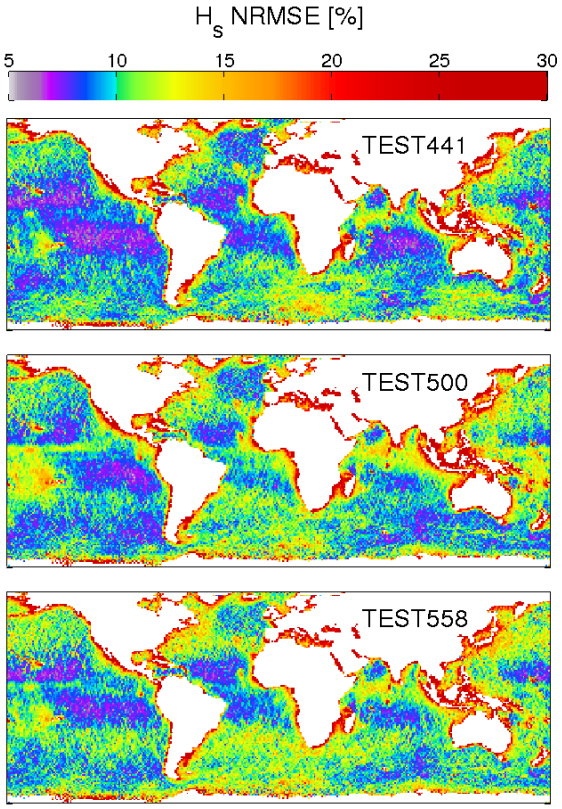

Fig. 4 : Comparison between significant wave height fields produced by parameterizations in WAVEWATCH III $^{(R)}$and wave height fields derived from altimeter observation for entire 2009 year.

So far, the three parameterizations, TEST441b, TEST500 and TEST558, produced fairly similar results in spite of very different source terms, with, in particular, opposite ratios of spontaneous and cumulative breaking. Because the distribution of wave breaking crest lengths Λ is directly link to breaking probabilities, we now use use observed distributions

of Λ, and other breaking statistics, to test the realism of the different parameterizations.

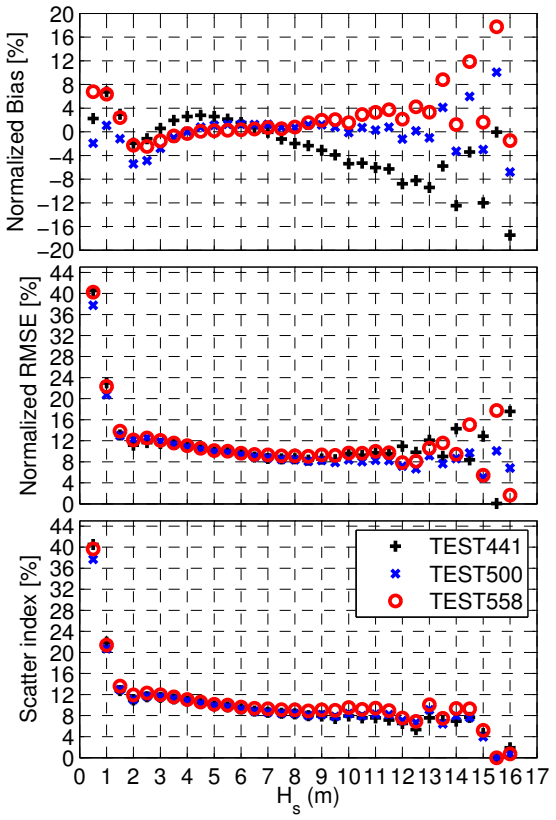

Fig. 5 : Bias, NRMSE and Satter Index for each parameterization in same condition as figure 4.

4 Whitecap Proprieties

We investigate in this part the modeling of whitecap proprieties. The parameterization TEST500 considers two opposite dissipations for spontaneous breaking and cumulative effect. Because of this inconstancy, this parameterization is not investigated further and we focus on TEST441b and TEST558. For TEST441b, breaking probabilities are extracted only from the direction-dependent saturation used to compute cumulative effect.

4.a Breaking Crest Lenght Distribution

Consistent with cumulative effect, Breaking Crest Length Distribution is defined by Eq. 6. Model runs starting from rest over uniform infinite deep ocean described above forced by 5ms^{-1}, 10ms^{-1} and 15ms^{-1} wind speeds. Spectrum and Breaking Wave Front Distribution $\Lambda(c)$ are shown on figure 6 for young and developed sea state. Both parameterizations show decreasing breaking crest length with sea state development. TEST441b produces a distribution shape equal to the saturation shape ; oversaturated smallest wave scales involve high breaking wave length densities. Density exponentialy decreases to the longer waves. The local increasing of breaking crest length density around the peak is consistent with observations of saturation spectrum by Banner et al. [2002]. Distributions are consistent with ones modeled for a sea state at statistical equilibrium [Phillips, 1985, Reul and Chapron, 2003].

The step around the peak is also produced by TEST558 on young sea state, but smoothed by wave scale analysis, and disappears on developped sea. However, this paraterization produces a BCLD with a distinct shape. First, it allows breaking of waves longer than peak wavelength, where saturation is under the threshold used in TEST441b. On the other hand, increasing of breaking crest length density with shorter waves is limited by an asymptotic value. Shapes of $\Lambda(c)$ distributions are consistent with wind-driven empirical models reported by Melville and Matusov [2002], but values are higher for a factor 10, corresponding to too high breaking probabilities.

4.b Whitecap coverage

Whitecap coverage is the fraction of sea surface affected by active breaking and static foam . The growth and decay rate of unsteady whitecaps were studied by several authors in terms of the temporal evolution of the area covered at the surface by individual whitecaps. Works by Kennedy and Snyder [1983] and Koepke [1984] give support to a monotonic increase of the whitecap size during stage A and an exponential character of foam field decay in stage B was clearly measured by Sharkov [1995] from analysis of time patterns of individual foam spot dissipation. Sea surface affected by each stage can be writen as the product of the length of breaking front times a fraction of the wavelength [Reul and Chapron, 2003]. These fractions can also be interpreted as the persistence time of each stage normalized by the wave period.

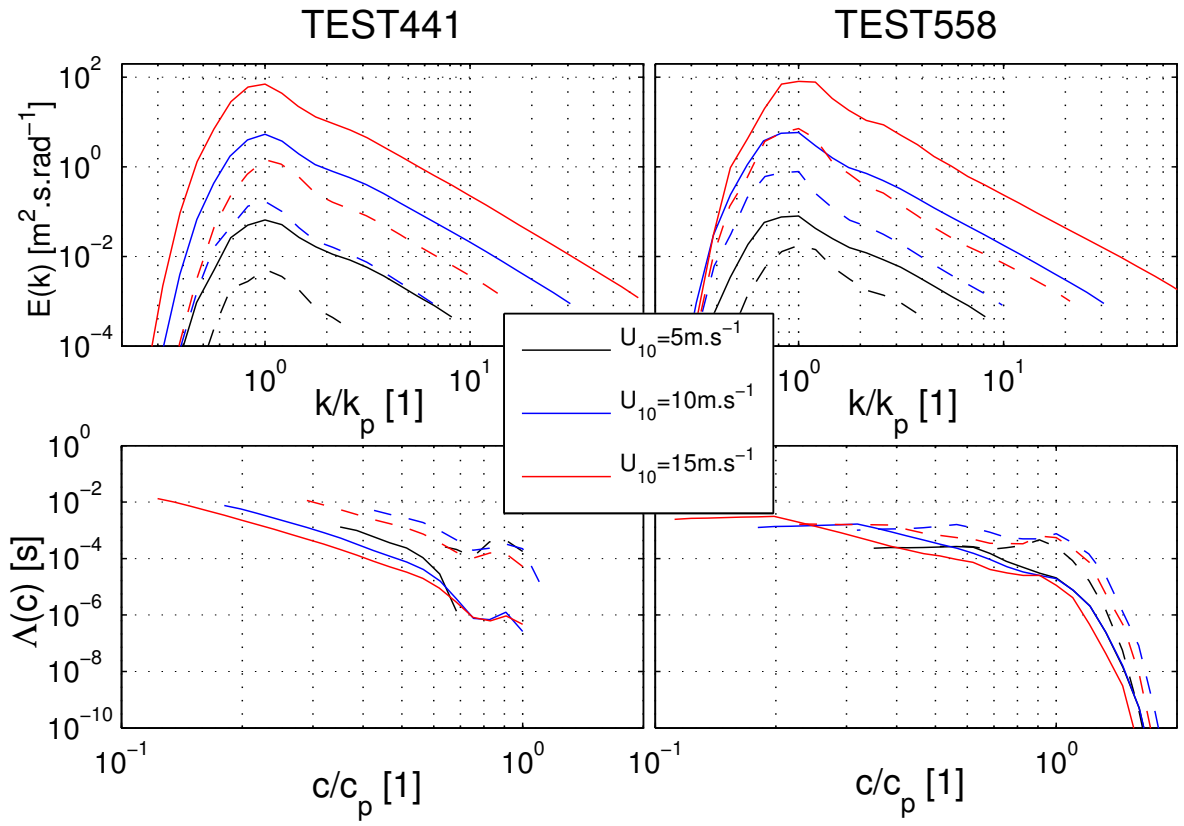

Fig. 6 : Top: spectrum function of non dimensional parameter k/k_p for 5ms^{-1} (black), 10ms^{-1} (blue) and 15ms^{-1} (red) wind speed for $c_\mathrm{p}/U_{10} < 1$ (dotted line) and $c_\mathrm{p}/U_{10} \sim 1$ (thin line). Bottom: corresponding modeled BCLD $\Lambda(c)$ function of non dimensional parameter c/c_p.

In this work, we propose to group the two stages using a mean whitecap width L_w,

$$L_w = \kappa \lambda_b, \tag{9}$$

consistent with a mean time persistence τ_p,

$$\tau_p = \kappa T_b, \tag{10}$$

where λ_b and T_b are wavelength and period of the breaker, respectively. The area covered by foam from each breaking event is the length of the associated breaking times the mean whitecap width defined above.

Length of breaking front generated by waves with velocities within the range c to $c+\mathrm{d}c$ is $\Lambda(c)\mathrm{d}c$. Therefore, the global whitecap coverage W produced by all breaking waves, is

$$W = \int_0^\infty \tau_p(c) c \Lambda(c) \mathrm{d}c \tag{11}$$

$$= \int_0^\infty \kappa \lambda_b(c) \Lambda(c) \mathrm{d}c, \tag{12}$$

In deep water, wavelength are proportional to the square of phase speed ($\lambda(c) = 2\pi c^2/g$) and whitecap coverage from breaking wave with velocities in the range c to $c + \mathrm{d}c$ is proportional to the second moment of $\Lambda(c)$ [Reul and Chapron, 2003].

κ is taken to give whitecap coverage in the range of observations. We propose $\kappa = 0.35$ for TEST441b and $\kappa = 0.15$ for TEST558. Fig. 7 shows the wind-dependence of modeled coverage for global 1-degree model on the entire year 2010. TEST441b implies a linear wind-dependence of the whitecap coverage, whereas TEST558 is proportional to U_{10}^2, in agreement with Monahan and Woolf [1989]. For both parameterizations, low values of coverage are computed for wind speeds under 5ms^{-1}. The high breaking probabilities that we modeled in TEST558 may account for the low value of κ. TEST441b show a linear wind-dependence whereas TEST558 exhibits a dependence in U_{10}^2, in consistency with Monahan and Woolf [1989].

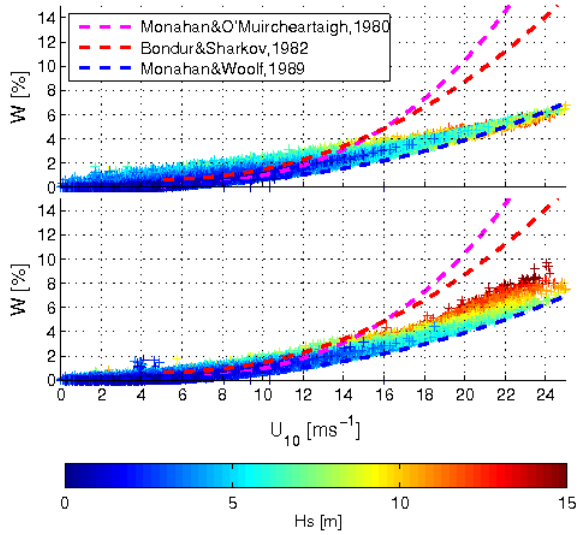

Fig. 7 : Whitecap coverage modeled in deep water with TEST441b (top) and new TEST558 (bottom) parameterization on 12/02/2010. Some wind-driven empirical fits are also plotted.

4.c Mean Foam Layer Thickness

Using model of the average vertical thickness of foam-layers proposed by Reul and Chapron [2003] (Fig.3, Eq.5), we propose an estimation of the mean thickness of the foam-layer. Time evolution of the average vertical thickness of foam-layers is split into stage A and B of breaking. During active breaking (stage A), vertical thickness grows linearly (equation 13) to reach a maximum value $\overline{\delta_{\max}}$. Then, foam thickness exponentially decreases with an exponential time constant τ' (stage B) to become infinitesimal (equation 14). Following Reul and Chapron [2003], the persistence time of active breaking is set to $0.8T_b$ and global persistence of a foam-layer, including stage A and B is set to $5T_b$ with T_b the period of the breaker. Time evolution of foam thickness $\overline{\delta}(c,t)$ for a wave with phase speed c is estimated for $0 < t < 0.8T_b$ using

$$\overline{\delta}(c,t) = \beta(\lambda_b)t \tag{13}$$

and for $0.8T_b < t < 5T_b$ using

$$\overline{\delta}(c,t) = \overline{\delta_{\max}}(\lambda_b)\exp\left(-\frac{t-0.8T_b}{\tau'}\right) \tag{14}$$

where the relaxation time τ' is equal to 3.8 (salt water). Time evolution of vertical thickness is integrated over the foam time persistence to obtain mean foam thickness $\overline{\Delta}(c)$ of individual breaking events. Integration of the whitecap coverage produced by each scale times its mean foam thickness over all wave scales gives a global mean foam thickness

$$\overline{\Delta} = \int_0^\infty \overline{\Delta}(c)\kappa\lambda_b(c)\Lambda(c)\mathrm{d}c, \tag{15}$$

with

$$\overline{\Delta}(c) = \int_0^{5T_b} \overline{\delta}(c,t)\mathrm{d}t. \tag{16}$$

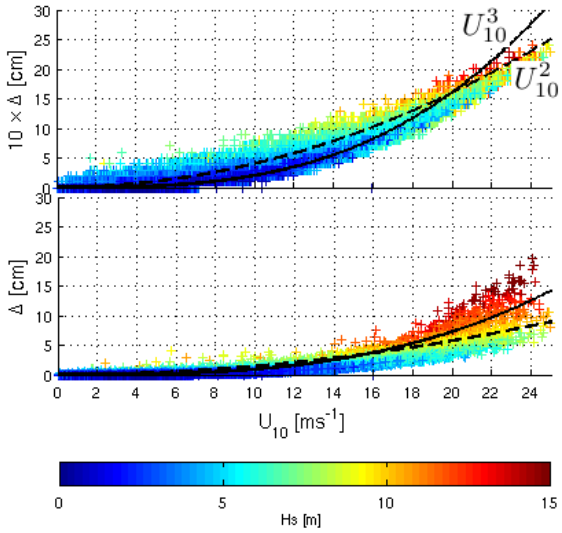

Fig. 8 : Mean foam thickness modeled in deep water with TEST441b (top) and new TEST558 (bottom) parameterization on entire year 2010.

Opposite wavelength distributions of breakers provide modeled mean foam thickness in TEST558 larger than in TEST441b by a factor 10. TEST441b leads to a dependence of the mean foam thickness in U_{10}^2 whereas TEST558 leads to a dependence in U_{10}^3. Moreover, breaking of shortest waves in TEST441b generates a important scatter at low wind speed and spreading decreases at stronger winds whereas breaking of wave around the peak induces an important dependence on wave age with strong winds.

5 Conclusion and Perspectives

Compared to the two previous parameterizations, TEST558 that is presented here accounts for the physical relation that intrinsically links spontaneous breaking and cumulative effect. In addition, the modeled whitecap properties are now closer to the observed ones. However, comparison with SHOWEX campaign data (not shown here) shows that TEST558 produced spectra overly narrow,

which is certainly due to the use of isotropic dissipation rate. Moreover, TEST441b provided a better fit with measured significant wave heights and spectral directional spreading. Performance at global scale of TEST441b implies that breaking dissipation is anisotropic, which could be due to an anisotropic distribution of breaking events. However, previous validations could only control the net source term $S_{tot} = S_{\rm in} + S_{\rm nl} + S_{\rm br}$ and there are likely compensating errors in TEST441b. In particular, it is well known that $S_{\rm nl}$ is not well parametrized by the DIA [Banner and Young, 1994, Ardhuin et al., 2007].

Finally, if breaking event induces an energy sink by turbulence, it also causes a modification of sea surface, which corresponds in the spectral domain to a redistribution of the energy. This effect is probably absorbed in the dissipation term of TEST441b that was semi-empirically determined.

Modeling of whitecap properties offers a new way to calibrate and validate dissipation source term in models at local scale with local observation of distribution of breaking wave crests [Melville and Matusov, 2002] and whitecap coverage [Mironov and Dulov, 2008] and at large scale with global observations from satellite [Anguelova and Webster, 2006].

Wave scale analysis of breaking proposed by Filipot et al. [2010] applied on stereo-video acquisitions should provide informations about breaking directionality and could enable observation of local modification of the sea surface by breaker.

References

M. D. Anguelova and F. W. Webster. Whitecap coverage from satellite measurements: a first step toward modeling the variability of oceanic whitecaps. *J. Geophys. Res.*, 111:C03017, 2006.

F. Ardhuin, T. H. C. Herbers, K. P. Watts, G. P. van Vledder, R. Jensen, and H. Graber. Swell and slanting fetch effects on wind wave growth. *J. Phys. Oceanogr.*, 37(4):908–931, 2007. doi: 10.1175/JPO3039.1.

F. Ardhuin, L. Marié, N. Rascle, P. Forget, and A. Roland. Observation and estimation of Lagrangian, Stokes and Eulerian currents induced by wind and waves at the sea surface. *J. Phys. Oceanogr.*, 39(11):2820–2838, 2009. URL `http://ams.allenpress.com/archive/2541-2558/39/11/pdf/i1520-0485-39-11-2820.pdf`.

F. Ardhuin, E. Rogers, A. Babanin, J.-F. Filipot, R. Magne, A. Roland, A. van der Westhuysen, P. Queffeulou, J.-M. Lefevre, L. Aouf, and F. Collard. Semi-empirical dissipation source functions for wind-wave models: part I, definition, calibration and validation. *J. Phys. Oceanogr.*, 40(9):1917–1941, 2010.

F. Ardhuin, A. Balanche, and E. Stutzmann. From seismic noise to ocean wave parameters: methods. *J. Geophys. Res.*, 2011. submitted.

M. L. Banner and R. P. Morison. Refined source terms in wind wave models with explicit wave breaking prediction. part I: Model framework and validation against field data. *Ocean Modelling*, 33:177–189, 2010. doi: 10.1016/j.ocemod.2010.01.002.

M. L. Banner and I. R. Young. Modeling spectral dissipation in the evolution of wind waves. part I: assessment of existing model performance. *J. Phys. Oceanogr.*, 24(7):1550–1570, 1994. URL `http://ams.allenpress.com/archive/1520-0485/24/7/pdf/i1520-0485-24-7-1550.pdf`.

M. L. Banner, I. S. F. Jones, and J. C. Trinder. Wavenumber spectra of short gravity waves. *J. Fluid Mech.*, 198: 321–344, 1989.

M. L. Banner, A. V. Babanin, and I. R. Young. Breaking probability for dominant waves on the sea surface. *J. Phys. Oceanogr.*, 30:3145–3160, 2000. URL `http://ams.allenpress.com/archive/1520-0485/30/12/pdf/i1520-0485-30-12-3145.pdf`.

M. L. Banner, J. R. Gemmrich, and D. M. Farmer. Multiscale measurement of ocean wave breaking probability. *J. Phys. Oceanogr.*, 32:3364–3374, 2002. URL `http://ams.allenpress.com/archive/1520-0485/32/12/pdf/i1520-0485-32-12-3364.pdf`.

J. Bidlot, S. Abdalla, and P. Janssen. A revised formulation for ocean wave dissipation in CY25R1. Technical Report Memorandum R60.9/JB/0516, Research Department, ECMWF, Reading, U. K., 2005.

J.-F. Filipot. *Parameterization of wave breaking and spectral modeling of sea states*. PhD thesis, Université Européenne de Bretagne, Ecole doctorale des Sciences de la Mer, Brest, France, 2010.

J.-F. Filipot, F. Ardhuin, and A. Babanin. A unified deep-to-shallow-water wave-breaking probability parameterization. *J. Geophys. Res.*, 115:C04022, 2010. doi: 10.1029/2009JC005448.

S. Hasselmann, K. Hasselmann, J. Allender, and T. Barnett. Computation and parameterizations of the nonlinear energy transfer in a gravity-wave spectrum. Part II: Parameterizations of the nonlinear energy transfer for application in wave models. *J. Phys. Oceanogr.*, 15:1378–1391, 1985. URL `http://ams.allenpress.com/archive/1520-0485/15/11/pdf/i1520-0485-15-11-1378.pdf`.

P. A. E. M. Janssen, A. C. M. Beljaars, A. Simmons, and P. Viterbo. The determination of the surface stress in an atmospheric model. *Mon. Weather Rev.*, 120:2977–2985, 1992.

R. M. Kennedy and R. L. Snyder. On the formation of whitecaps by a threshold mechanism. part II: Monte Carlo experiments. *J. Phys. Oceanogr.*, 13:1493–1504, 1983.

P. Koepke. Effective reflectance of oceanic whitecaps. *Appl. Opt.*, 23(11):1816–1824, 1984. doi: 10.1364/AO.23.001816. URL `http://ao.osa.org/abstract.cfm?URI=ao-23-11-1816`.

W. K. Melville and P. Matusov. Distribution of breaking waves at the ocean surface. *Nature*, 417:58–63, 2002.

A. S. Mironov and V. A. Dulov. Detection of wave breaking using sea surface video records. *Meas. Sci. Technol.*, 19: 015405, 2008.

E. C. Monahan and D. K. Woolf. Comments on "variations of whitecap coverage with wind stress and water temperature". *J. Phys. Oceanogr.*, 19:706–709, 1989. URL `http://ams.allenpress.com/archive/1520-0485/19/5/pdf/i1520-0485-19-5-706.pdf`.

O. M. Phillips. On the response of short ocean wave components at a fixed wavenumber to ocean current variations. *J. Phys. Oceanogr.*, 14:1425–1433, 1984. URL `http://ams.allenpress.com/archive/1520-0485/14/9/pdf/i1520-0485-14-9-1425.pdf`.

O. M. Phillips. Spectral and statistical properties of the equilibrium range in wind-generated gravity waves. *J. Fluid Mech.*, 156:505–531, 1985.

P. Queffeulou and D. Croizé-Fillon. Global altimeter SWH data set, version 7, may 2010. Technical report, Ifremer, 2010.

N. Reul and B. Chapron. A model of sea-foam thickness distribution for passive microwave remote sensing applications. *J. Geophys. Res.*, 108(C10):3321, 2003. doi:10.1029/2003JC001887.

Y. A. Sharkov. Experimental investigations of the lifetime for breaking wave dispersive zone. *Izv. Atmos. Oceanic Phys.*, 30(11):808–811, 1995.

E. B. Thornton and R. T. Guza. Transformation of wave height distribution. *J. Geophys. Res.*, 88(C10):5,925–5,938, 1983.

H. L. Tolman. A mosaic approach to wind wave modeling. *Ocean Modelling*, 25:35–47, 2008. doi: 10.1016/j.ocemod.2008.06.005.

H. L. Tolman and D. Chalikov. Source terms in a third-generation wind wave model. *J. Phys. Oceanogr.*, 26: 2497–2518, 1996.

A. J. van der Westhuysen, M. Zijlema, and J. A. Battjes. Saturation-based whitecapping dissipation in SWAN for deep and shallow water. *Coastal Eng.*, 54:151–170, 2007.

WISE Group. Wave modelling - the state of the art. *Progress in Oceanography*, 75:603–674, 2007. doi: 10.1016/j.pocean.2007.05.005.

I. R. Young and A. V. Babanin. Spectral distribution of energy dissipation of wind-generated waves due to dominant wave breaking. *J. Phys. Oceanogr.*, 36:376–394, 2006.